Interplay between spin-density wave and induced local moments in URu_2Si_2

V. P. Mineev and M. E. Zhitomirsky
Commissariat á l'Energie Atomique, DSM/DRFMC/SPSMS 38054 Grenoble, France
(Received 2 December 2004; revised manuscript received 23 February 2005; published 14 July 2005)

Theoretical model for magnetic ordering in the heavy-fermion metal URu_2Si_2 is suggested. The 17.5 K transition in this material is ascribed to formation of a spin-density wave (SDW), which develops due to a partial nesting between electron and hole parts of the Fermi surface and has a negligibly small form factor. Staggered field in the SDW state induces tiny antiferromagnetic order in the subsystem of localized singlet-singlet levels. Unlike the other models, our scenario is based on coexistence of two orderings with the same antiferromagnetic dipole symmetry. The topology of the pressure phase diagram for such a two-order parameter model is studied in the framework of the Landau theory. The field dependences of the staggered magnetization and the magnon gap are derived from the microscopic theory and found to be in good quantitative agreement with experiment.

DOI: 10.1103/PhysRevB.72.014432 PACS number(s): 71.27.+a, 75.10.−b, 75.30.Fv

I. INTRODUCTION

URu_2Si_2 is one of the most intriguing heavy-fermion compounds. It exhibits a sharp second-order transition at $T_m=17.5$ K, which has a pronounced effect on thermodynamic and kinetic properties,[1–5] though the neutron diffraction experiments[6–9] and the x-ray magnetic scattering measurements[10] have produced evidence for only tiny staggered moments $\mu \simeq 0.02-0.04\mu_B$ at $\mathbf{Q}=(1,0,0)$. Magnetic excitations observed by inelastic neutron scattering experiments[6,8] are reasonably well explained within the model with exchange interaction in a singlet-singlet Van Vleck paramagnet.[11] This model fails, however, to give a consistent description of the ordering temperature and small ordered moments unless the exchange interaction $\mathcal{J}_{\mathbf{Q}}$ is accidentally close to a critical value (see Sec. IV below). A weak antiferromagnetic ordering of a Van Vleck paramagnet cannot produce a measured jump in the specific heat[3] and an electrical resistivity anomaly.[4] These experimental features rather resemble formation of a spin-density wave (SDW), which involves approximately half of the Fermi surface. In its turn, the SDW scenario is inconsistent with a longitudinal polarization of the magnetic excitations. As a result of this contradiction, various theoretical scenarios have been proposed in the past to explain intriguing behavior of URu_2Si_2.[12–23]

The proposed theories of URu_2Si_2 can be crudely divided into three broad categories. Phenomenological models of the first group[15,20] take a pragmatic approach and introduce a yet unknown primary or hidden order parameter ψ, which drives the 17.5 K transition and is responsible for a large specific heat anomaly at T_m. Small ordered moments observed in the neutron experiments are described by a secondary Ising-like antiferromagnetic order parameter m. Depending on the symmetry of the hidden order parameter, different coupling terms of the type ψm and $\psi^2 m^2$ are possible in the Landau energy functional. In particular, the model with a bilinear term predicts a nontrivial field dependence of weak antiferromagnetic moments with an inflection point.[20] Subsequent neutron measurements have nicely confirmed such a prediction.[24]

A second group of theories consists of specific proposals for the hidden order parameter. These models are further subdivided into two subgroups. The first subgroup includes models, in which the primary order parameter breaks the time-reversal symmetry. These are spin-density waves in higher angular momentum channels,[13,19] triple spin correlators,[12,15] orbital antiferromagnetism,[21] and ordering of octupolar moments on uranium sites.[22] For such theories the bilinear coupling term with the antiferromagnetic vector is, in principle, possible, though some other crystal symmetries are required to be absent. The second subgroup includes theoretical models with a time-reversal invariant hidden order parameter such as quadrupolar[16] or spin nematic ordering.[14] In such a case the bilinear term is prohibited by symmetry and only a biquadratic interaction exists between the two-order parameters.

The last third group of theoretical works includes attempts to realistically describe the microscopic interactions in URu_2Si_2. A so-called Ising–Kondo lattice model[17] describes interaction between conduction electrons in nested bands and local crystal-field split moments. The mean-field calculation produces both a weak moment and an appropriate value of the transition temperature but does not reproduce the large specific heat jump. A closely related dual model[18] considers a subsystem of localized singlet-singlet levels and a subsystem of itinerant electrons with a similar assumption on the nesting condition. A better description of the thermodynamic properties of URu_2Si_2 has been achieved by adding the superexchange and the Ruderman-Kittel-(Kasuya)-Yosida (RK(K)Y) interactions between local moments. The field behavior still remains largely inconsistent with the experimental measurements.[24] Further development of the dual model has been recently suggested in Ref. 23. Note, that the above two microscopic models (i) completely neglect the Coulomb interaction between charge carriers and (ii) operate with a single (antiferromagnetic) order parameter.

Up to now experiments have been unable to distinguish between the competing theoretical proposals. Two potentially important experimental developments published recently include pressure experiments and the nuclear magnetic resonance (NMR) measurements. Investigations under hydro-

 ©2005 The American Physical Society

static pressure[25–27] have shown that the P-T phase diagram is divided into two regions: a small moment antiferromagnetic phase (SMAF) at low pressures and a large moment antiferromagnetic phase (LMAF) at high pressures with a first-order transition line in between. Such a discovery is generally consistent with phenomenological two-order parameter scenarios for URu_2Si_2 (see Sec. III, below). Another experimental finding came out of the NMR measurements. Matsuda and co-workers[28,29] have found that a paramagnetic Si^{29} NMR absorption line persists well below T_m accompanied by two much smaller peaks symmetrically shifted by antiferromagnetic field. Such an observation points at an inhomogeneous para-antiferromagnetic state below the 17.5 K transition. The peak intensities suggest that about 97% of the sample volume is in a paramagnetic state. The puzzle of small uranium moments in URu_2Si_2 seems to be reinterpreted as due to a phase separation between nonmagnetic state with a hidden order and small antiferromagnetic droplets with ordinary (large) value of staggered magnetization. Such a simple explanation of the main mystery of URu_2Si_2 is quite appealing but leaves without answering the question why the inhomogeneous phase exists not only in the vicinity of the first-order transition line at high pressures, but in the whole region of SMAF. The development of the antiferromagnetic Bragg peaks right below $T_m=17.5$ K seems to be highly accidental in the phase separation scenario. Also, an inflection point in the field dependence of antiferromagnetic Bragg peaks cannot be explained if small peaks are purely due to a volume effect. Thus, physical implications of the NMR measurements[28,29] are not completely straightforward and have to be further clarified.

In this paper, we present a semimicroscopic model for URu_2Si_2, which is closely related to the abovementioned dual models,[17,18] but operates with two-order parameters in the spirit of phenomenological scenarios.[15,20] We also consider two magnetic subsystems: (i) local crystal-field split moments on U^{4+} sites and (ii) conduction electrons in nested bands. In contrast to the previous works[17,18] we assume that the electron-electron interaction is non-negligible and that it drives a SDW transition in the nested parts of the Fermi surface. The critical temperature $T_m=17.5$ K is associated with T_{SDW} and the SDW amplitude ψ plays the role of a primary (hidden) order parameter. According to the local spin density approximation calculations[30] the nesting wave vector is commensurate and corresponds to the experimentally observed two-sublattice antiferromagnetic structure. The SDW formed in conduction bands is responsible for large changes in thermodynamic and kinetic properties of URu_2Si_2. At the same time, we argue that the SDW has a small form factor and does not create significant Bragg reflection. Local polarization of uranium sites by a staggered magnetic field from the SDW induces tiny antiferromagnetic moments. The magnetic dynamics probed by neutrons is also determined by a localized subsystem.

By making a single assumption about a hidden order parameter with the same symmetry as the observed antiferromagnetic ordering, we have further derived several results, which allow detailed comparison with available measurements and suggest future experimental tests:

(i) the P-T phase diagram with line of the first-order-type transition, which terminates at the critical point below $T_m(P)$;

(ii) field dependence of staggered magnetization coincides perfectly with the experimental data for a realistic set of microscopic parameters; and

(iii) field dependence of the excitation spectrum.

The article is organized as follows. In Sec. II, we introduce the model and discuss various features of the spin-density wave instability specific for URu_2Si_2. In Sec. III, using the phenomenological approach with an appropriate Landau energy functional for two coexistent order parameters, we investigate the topology of the P-T phase diagram of URu_2Si_2. In the next section, a system of localized crystal-field split singlet-singlet levels is considered under combined influence of a uniform external magnetic field and a staggered "internal" field induced by the SDW. We calculate the field dependences of the staggered magnetization and the excitation spectrum. Comparison to the experimental data is presented in Sec. V, which is followed by discussion and conclusions.

II. SPIN-DENSITY WAVE

An unusual assumption made by phenomenological theories[15,20] is a description of URu_2Si_2 with two-order parameters having the same symmetry. On the first site such an assumption contradicts to a general spirit of the Landau theory of phase transition. Recent investigations of a two-gap superconductor MgB_2 have, however, demonstrated usefulness of the description of the superconducting state by means of two weakly interacting s-wave condensates of the Cooper pairs (see, for instance, Ref. 31). The necessary condition for this is a significant mismatch of the pairing interactions in the two bands. In the absence of interband scattering of the Cooper pairs, each band has its own superconducting transition temperature. An interband interaction is always present in real metals and leads to a single transition into a state with two different gaps. The two gaps (order parameters) still keep different dependences on temperature, pressure and/or applied magnetic field. In relation to URu_2Si_2, the two-order parameters ψ and m should correspond to two significantly different magnetic subsystems. We suggest here that the primary order parameter may be an ordinary SDW. The common objections against a SDW transition are (i) smallness of ordered moments and (ii) longitudinal polarization of sharp magnetic excitations. These two properties can be reconciled with a SDW scenario by taking into account specific features of URu_2Si_2. In this section we discuss the former feature, while the properties of magnetic excitations are considered in Sec. IV.

The early experimental works on the specific heat[3,32] and the magnetoresistance[4] in URu_2Si_2 have found strong evidences in favor of charge or spin-density wave instabilities in the heavy-electron subsystem at $T_m=17.5$ K. The fit of the electronic specific heat below the transition indicates that a gap $\Delta_0\simeq 130$ K develops on 40% of the Fermi surface at $T\rightarrow 0$. This conclusion has received strong support from the de Haas–van Alphen (dHvA) measurements.[33] Comparison of the measured dHvA frequencies to the *ab initio* band structure shows that two large pieces of the Fermi surfaces,

band-18 hole and band-19 electron, are not observed at low temperatures, probably due to their partial removal below the ordering temperature. The above two sheets have nearly spherical shapes and are separated by a nesting wave vector $\mathbf{Q}=(0,0,1)$, which is equivalent to (1, 0, 0) in the Brillouin zone of a body-centered tetragonal lattice.[33] Direct calculation of a static momentum-dependent susceptibility[30] also shows a peak at the commensurate wave vector $\mathbf{Q}=(1,0,0)$.

A fast decrease of the uniform susceptibility[13] below T_m as well as suppression of the transition temperature T_m and the bulk gap Δ_0 by applied magnetic field[34–36] also point to a charge- or a spin-density wave state. For the charge density wave the Zeeman splitting degrades the nesting of the Fermi surfaces and reduces a mean-field transition temperature[37] in a way which is analogous to the paramagnetic limit effect in superconductors. By contrast, an isotropic SDW involves coupling of bands with opposite spin and the nesting is not affected by a magnetic field. A strong spin-orbit coupling in heavy-fermion materials creates momentum dependence of the g factor. If the nesting condition $\varepsilon(\mathbf{k}+\mathbf{Q})=-\varepsilon(\mathbf{k})$ is satisfied for particular sheets of the Fermi surface it is not generally fulfilled for the Zeeman shift $\mu_B g(\mathbf{k}+\mathbf{Q})H/2 \neq \mu_B g(\mathbf{k})H/2$. Hence, in metals with strong spin-orbit coupling a SDW state is also suppressed by the paramagnetic effect.

The mean-field theory of a SDW formation in ideally nested electron and hole Fermi surfaces[38] resembles to a large extent the Bardeen–Cooper–Schrieffer (BCS) theory. The relative jump of the specific heat at $T_m=T_{\mathrm{SDW}}$ is estimated by the BCS value $\Delta C/C\simeq 1.43$, which is compatible with the experimental value $\Delta C/C\approx 2.9$ once additional strong-coupling effects are taken into account. The modulation of the spin density at $T=0$ is given by

$$M_{\mathbf{Q}}^{z}=\mu_B\sum_{\mathbf{k}}\langle c_{\mathbf{k}+\mathbf{Q}\uparrow}^{\dagger}c_{\mathbf{k}\uparrow}\rangle=\mu_B N_0\Delta_0\ln\frac{\varepsilon_F}{\Delta_0}, \qquad (1)$$

where N_0 is the density of states per one spin direction. Estimating $N_0\simeq n_e/\varepsilon_F$, we find that ordered moments normalized per 1 constitute a small fraction of the Bohr magneton $\sim\Delta_0/\varepsilon_F$.[38] Such a reduction has a transparent physical meaning: only electrons (holes) within a thin layer of width $2\Delta_0$ around the Fermi surface participate in the formation of ordered moments. Thus, affecting strongly thermodynamic and kinetic properties, a weak-coupling SDW order has a small form factor and does not produce significant magnetic Bragg scattering. This fact has not been so far appreciated in the literature on URu_2Si_2.

There are several additional factors, which complicate the simple picture drawn above. First, the perfect nesting between different bands does not appear in real materials. Absence of perfect nesting acts as a depairing effect reducing gradually both the transition temperature and the zero-T gap and enhancing the residual density of states. Obviously, such an effect does not change the conclusion about a small form factor, but may reduce the jump in the specific heat compared to the BCS value. In order to show that partial nesting does not modify the previous estimate, we refer to a similar situation in superconductors with paramagnetic (depairing) impurities. Using the Abrikosov–Gor'kov theory, Skalski, Betbeder-Matibet, and Weiss[39] have calculated the effect of paramagnetic impurities on various characteristics of an s-wave superconductor. Their results indicate that in a wide range of impurity concentration, the jump in the specific heat and the transition temperature are suppressed at approximately the same rate, hence, preserving the BCS estimate for the relative specific heat jump. Second, the electron mass enhancement in heavy-fermion materials ($m^*/m\sim 25$ in URu_2Si_2) can significantly reduce the Fermi energy scale ε_F. However, simultaneously with a mass renormalization, an interaction with spin fluctuations strongly reduces the spectral weight of heavy quasiparticles[40,41] adding an extra small factor $(m/m^*)^3$ to Eq. (1), which completely compensates the factor (m^*/m) in the density of states and further reduces value of the ordered moments. Finally, according to the band structure calculations[30,33] URu_2Si_2 is a compensated metal with equal number of electrons and holes. The number of carriers in the two bands undergoing a SDW transition is smaller than one, when normalized to the number of U atoms. This yields an extra reduction factor, since the neutron scattering experiments report the ordered moments normalized per one uranium.

The above arguments can, in our view, convincingly explain why small antiferromagnetic Bragg peaks in URu_2Si_2 are consistent with a SDW instability. In the following we assume that due to nesting between some parts of the Fermi surface in URu_2Si_2 the commensurate SDW state is formed below the critical temperature T_m and that the SDW amplitude $\psi\sim\Sigma_{\mathbf{k}}\langle c_{\mathbf{k}+\mathbf{Q}\uparrow}^{\dagger}c_{\mathbf{k}\uparrow}\rangle$ plays the role of a hidden order parameter in the problem.

III. PHASE DIAGRAM UNDER PRESSURE

The microscopic dual models[17,18] assume that conduction electrons are noninteracting and operate, therefore, with a single order parameter, which leaves no place for the phase diagram with SMAF and LMAF regions. In our scenario, temperatures of intrinsic phase transitions in itinerant and localized magnetic subsystems are different functions of P and they may interchange their order under pressure. As a result, a line of first-order transitions appears naturally between the two ordered states, where one order parameter prevails over another, see Fig. 1.

The Landau free energy for two interacting order parameters can be written as

$$F=\alpha_1\psi^2+\alpha_2 m^2+2\gamma\psi m+\beta_1\psi^4+\beta_2 m^4+2\beta_i\psi^2 m^2. \quad (2)$$

A special bilinear coupling term is allowed only if the two parameters transform according to the same irreducible representation, otherwise $\gamma\equiv 0$. For nonzero γ, the quantities ψ and m do not correspond to two different types of symmetry breaking. Rather they describe two weakly coupled magnetic subsystems of URu_2Si_2 in a way which is reminiscent of the Ginzburg–Landau description of the multigap superconductivity in MgB_2.[31] The bilinear term corresponds, then, to a polarization of local moments by a spin-density wave.

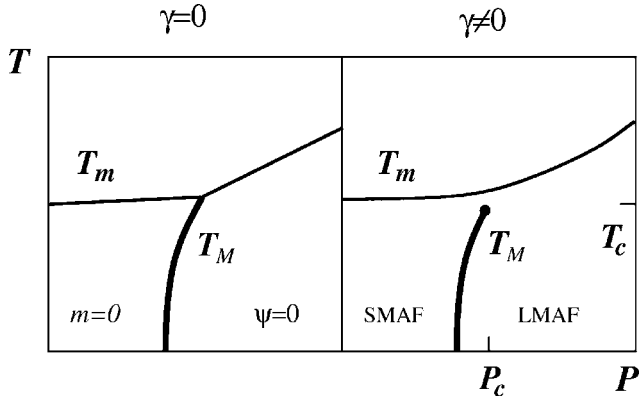

FIG. 1. The phase diagram of the two-order parameter Landau functional for $\gamma=0$ (left panel) and for $\gamma\neq 0$ (right panel).

Generally, in addition to the bilinear term ψm there are possible other coupling terms in the Landau functional: $\psi^3 m$ and ψm^3. These terms can exist even if ψ and m transform according to different irreducible representations (though ψ has to break the time-reversal symmetry). The $\psi^3 m$ term leads, for example, to a small antiferromagnetic component in a state with $\psi\neq 0$, even if $\gamma\equiv 0$. The induced m component grows in such a case as $m\sim(T_m-T)^{3/2}$, while the neutron diffraction experiments find a standard mean-field exponent $1/2$.[6,7] This observation suggests that the ψm coupling plays a dominant role and, hence, the phenomenological coefficients for $\psi^3 m$ and ψm^3 terms have the same smallness as γ. In such a case, a simple linear transformation allows to exclude such terms from the Landau functional without significantly modifying the physical meaning of ψ and m.

For $\gamma=0$ the functional (2) has a form commonly found in the theory of phase transitions. Assuming that only coefficients $\alpha_{1,2}$ depend on temperature and pressure, the energy (2) describes a phase diagram with two crossing lines of second-order transitions determined by $\alpha_{1,2}(P,T)=0$. The transition line from a paramagnetic state $T_m(P)$ has a kink at the crossing point. Presence and nature of extra transitions in the order state, where α_1, $\alpha_2<0$, depend on quartic terms. For $\beta_i<\sqrt{\beta_1\beta_2}$ or for a weak repulsion between ψ and m, there are two other lines of second-order transitions emerging from the crossing point. They separate two states with pure ordering, i.e., $\psi\neq 0$, $m=0$ and $\psi=0$, $m\neq 0$, from a mixed phase with $\psi\neq 0$ and $m\neq 0$. Thus, the phase diagram in this case has a tetracritical point. For $\beta_i>\sqrt{\beta_1\beta_2}$ or for a strong repulsion between two components, the mixed phase does not appear. Instead, there is a single line of first-order transitions in the P-T plane given by $\alpha_1^2\beta_2=\alpha_2^2\beta_1$, which approaches the kink (crossing) point from the ordered side, see the left panel in Fig. 1.

In the following we discuss effect of nonzero γ on the two-order parameter functional (2): problem, which, to our knowledge, has not been considered so far. Once $\gamma\neq 0$, the two-order parameters appear simultaneously on a single transition line given by $\alpha_1\alpha_2=\gamma^2$. The transition temperature from a paramagnetic state $T_m(P)$ has now a smooth pressure dependence and does not exhibit a kink. At $P=0$, the induced antiferromagnetic component behaves as

$$m\approx -(\gamma/\alpha_2)\psi \tag{3}$$

for $|\alpha_1|,|\gamma|\ll\alpha_2$. A small coefficient γ/α_2 implies weak ordered moments, while ψ gives rise to a large anomaly in the specific heat at T_m. We identify this phase with a small moment antiferromagnetic (SMAF) phase of URu_2Si_2.

In order to investigate the possible ordered states and phase transitions below $T_m(P)$, one has to minimize Eq. (2) with respect to both ψ and m. This gives a system of two coupled cubic equations, which is easily solved numerically, but does not allow full analytic solution. Still, simple analytic arguments can be used to prove stability of the first-order transition line for $\gamma\neq 0$ and $\beta_i>\sqrt{\beta_1\beta_2}$. [For $\beta_i<\sqrt{\beta_1\beta_2}$, the bilinear term stabilizes the mixed phase ($\psi\neq 0$ and $m\neq 0$) right below $T_m(P)$.]

Substitution $m\to(\beta_1/\beta_2)^{1/4}m$ transforms the free energy to a more symmetric form

$$F=\alpha_1\psi^2+\tilde{\alpha}_2 m^2+2\tilde{\gamma}\psi m+\beta_1(\psi^2+m^2)^2+2\tilde{\beta}_i\psi^2 m^2, \tag{4}$$

where $\tilde{\alpha}_2=(\beta_1/\beta_2)^{1/2}\alpha_2$, $\tilde{\gamma}=(\beta_1/\beta_2)^{1/4}\gamma$, and $\tilde{\beta}_i=(\beta_1/\beta_2)^{1/2}\beta_i-\beta_1$. In the new notations the condition for the absence of the mixed phase at $\gamma=0$ is $\tilde{\beta}_i>0$, while the position of the first-order transitions line in the P-T plane is given by $\alpha_1=\tilde{\alpha}_2$. Let us cross from the paramagnetic state into the ordered state along this line taking $\alpha_1=\tilde{\alpha}_2=\alpha$. The transformation $\psi=\eta_1-\eta_2$, $m=\eta_1+\eta_2$ diagonalizes the quadratic terms in Eq. (4) yielding

$$F=2(\alpha+\tilde{\gamma})\eta_1^2+2(\alpha-\tilde{\gamma})\eta_2^2+4\beta_1(\eta_1^2+\eta_2^2)^2+2\tilde{\beta}_i(\eta_1^2-\eta_2^2)^2. \tag{5}$$

If we assume, for example, $\gamma<0$, then a second-order transition takes place at $\alpha(T_m)=-\tilde{\gamma}$ from a paramagnetic state into a state with $\eta_1^2=-(\alpha+\tilde{\gamma})/2(2\beta_1+\tilde{\beta}_i)$, while $\eta_2=0$. For positive $\tilde{\beta}_i$, the last term in Eq. (5) disfavors states with $\eta_1^2\neq\eta_2^2$. Therefore, at sufficiently low temperature there should be another transition into a state with a nonzero η_2. The location of such a critical point (T_c,P_c) is given by

$$\alpha(T_c)=-2|\tilde{\gamma}|\frac{\beta_1}{\tilde{\beta}_i}=-\frac{2|\gamma|(\beta_1^3\beta_2)^{1/4}}{\beta_i-\sqrt{\beta_1\beta_2}}. \tag{6}$$

The ratio of the specific heat jumps at two consecutive transitions T_m and T_c is

$$\frac{\Delta(C/T)_c}{\Delta(C/T)_m}=\frac{\tilde{\beta}_i}{2\beta_1}. \tag{7}$$

For $\alpha<\alpha(T_c)$ the two components behave as

$$\eta_1^2=-\frac{\tilde{\beta}_i\alpha+2\tilde{\gamma}\beta_1}{8\beta_1\tilde{\beta}_i},\quad \eta_2^2=-\frac{\tilde{\beta}_i\alpha-2\tilde{\gamma}\beta_1}{8\beta_1\tilde{\beta}_i}. \tag{8}$$

The relative phase between η_1 and η_2 is not fixed, though solutions $(|\eta_1|,|\eta_2|)$ and $(|\eta_1|,-|\eta_2|)$ describe two essentially different states. Away from the line $\alpha_1=\tilde{\alpha}_2$, the energy (5) acquires the extra term $2(\alpha_1-\tilde{\alpha}_2)\eta_1\eta_2$, which immediately lifts the above twofold degeneracy and selects either 0 or π

shift between η_1 and η_2 on the two sides of $\alpha_1=\tilde{\alpha}_2$. Consequently, the first-order transition line $T_M(P)$ is stable and its position in the P-T plane is given by the same equation as for $\gamma=0$. However, $T_M(P)$ splits from the line of second-order phase transitions $T_m(P)$ and terminates at the critical point determined by Eq. (6), see the right panel of Fig. 1.

The two states to the left and to the right from $T_M(P)$ are phases with large $\psi_L=|\eta_1|+|\eta_2|$ and small $m_S=|\eta_1|-|\eta_2|$ (SMAF) and with small $\psi_S=|\eta_1|-|\eta_2|$ and large $m_L=|\eta_1|+|\eta_2|$ (LMAF). A relative jump of the ordered antiferromagnetic moments across $T_M(P)$ is given by

$$\frac{m_L-m_S}{m_L+m_S}=\frac{|\eta_2|}{|\eta_1|}=\sqrt{\frac{\alpha-\alpha(T_c)}{\alpha+\alpha(T_c)}}. \tag{9}$$

The size of the jump varies continuously along $T_M(P)$ and vanishes at $P=P_c$. Note that the distance between the critical line $T_m(P)$ and the critical point T_c given by Eq. (6) is proportional to γ and may be quite small. At present, the neutron experiments under hydrostatic pressure have failed to identify the critical end point (T_c,P_c) on the line of first-order transitions $T_M(P)$.[27] We suggest that specific heat measurements can help to finally resolve the phase diagram of URu_2Si_2.

IV. CRYSTAL-FIELD MODEL FOR INDUCED MOMENTS

The ninefold degenerate state of U^{4+} ions with the total angular momentum $J=4$ is split by a crystalline electric field. Following the previous work,[8,17,18] we assume that the ground and the first excited levels are singlets separated by a crystal field gap Δ and that the only nonvanishing matrix element of the total angular momentum is $\langle 0|J^z|1\rangle=\mu$. Working on the basis of the two lowest levels, the new pseudo-spin-1/2 operators are defined as

$$S^z|0\rangle=+\frac{1}{2}|0\rangle, \quad S^z|1\rangle=-\frac{1}{2}|1\rangle. \tag{10}$$

The nonzero component of the angular momentum operator is expressed in terms of pseudo-spin-1/2 operators as $J^z=2\mu S^x$. Local moments formed by the mixing of two crystal-field levels have, therefore, a very anisotropic nature. They couple only to a z component of an applied field and via Ising-like interaction between different sites. Coupling between local moments and itinerant carriers is described by an Ising–Kondo interaction[17]

$$\hat{V}=\frac{1}{2}I\sum_i J_i^z c_{i\alpha}^\dagger \sigma_{\alpha\beta}^z c_{i\beta}. \tag{11}$$

Below the SDW transition, space modulation of the electron spin density produces an internal staggered field on uranium sites

$$H_s(\mathbf{r}_i)=H_s e^{i\mathbf{Q}\mathbf{r}_i}, \quad H_s=-IM_{\mathbf{Q}}^z\sim\psi. \tag{12}$$

The estimate of the staggered field from the experimental data on URu_2Si_2 is given in Sec. V. Transformation from Eq. (11) to Eq. (12) corresponds to a mean-field approximation, which should be sufficient when considering two weakly interacting subsystems.

The total crystal-field Hamiltonian in the presence of both staggered and uniform fields applied parallel to the crystal $\hat{\mathbf{z}}$ axis is written in terms of pseudo-spin operators as

$$\hat{\mathcal{H}}=4\mu^2\sum_{\langle i,j\rangle}\mathcal{J}(ij)S_i^xS_j^x-\Delta\sum_i S_i^z-2\mu\sum_i(H+H_s e^{i\mathbf{Q}\mathbf{r}_i})S_i^x, \tag{13}$$

where $\mathcal{J}(ij)$ is a set of exchange constants between local moments on a body centered tetragonal lattice.

A. Zero-field case

The crystal-field model (13) in zero applied field has been studied by many authors.[42–46] The Hamiltonian (13) without the last term corresponds to a ubiquitous Ising model in a transverse field. In order to make connection with previous works we briefly list in this subsection the main results on the crystal-field model (13) with $H=H_s=0$. At zero temperature and in the large gap limit the system remains in a singlet ground state. The excitation spectrum consists of magnetic or Van Vleck excitons, which are bound states of the two singlet levels. Energy of Van Vleck excitons is easily found by applying the Holstein–Primakoff representation to pseudo-spin-1/2 operators. In the harmonic approximation it is suffice to write

$$S_i^z=\frac{1}{2}-a_i^\dagger a_i, \quad S_i^x=\frac{1}{2}(a_i^\dagger+a_i). \tag{14}$$

The excitation spectrum is given by

$$\omega_{\mathbf{k}}=\sqrt{\Delta(\Delta+2\mu^2\mathcal{J}_{\mathbf{k}})}, \tag{15}$$

where $\mathcal{J}_{\mathbf{k}}=\Sigma_j\mathcal{J}(ij)e^{i\mathbf{k}\mathbf{r}_{ij}}$ is a Fourier transform of the exchange interaction. The excitation gap is reduced by magnetic interactions to

$$\Delta_g=\sqrt{\Delta(\Delta-\Delta_c)}, \quad \Delta_c=2\mu^2|\mathcal{J}_{\mathbf{Q}}|, \tag{16}$$

where the wave vector $\mathbf{Q}$ corresponds to the absolute minimum of $\mathcal{J}_{\mathbf{k}}$. Let us emphasize here that neither Δ nor Δ_g have any relation to the bulk gap Δ_0, which corresponds to itinerant magnetic subsystem. Quantum fluctuations somewhat renormalize the spectrum (15) at $T=0$ and tend to further reduce the critical gap Δ_c.[44,45] This effect depends, however, on a particular form of $\mathcal{J}_{\mathbf{k}}$, and for a three-dimensional system does not exceed 2%–3%. Below, we neglect such quantum corrections.

If the crystal-field splitting Δ becomes smaller than Δ_c, the system develops a long-range magnetic order with a staggered magnetization $\langle J_i^z\rangle=2\mu\langle S_i^x\rangle\sim e^{i\mathbf{Q}\mathbf{r}_i}$. In the following we always assume that magnetic ordering has a two-sublattice antiferromagnetic structure, that is $e^{2i\mathbf{Q}\mathbf{r}_i}\equiv 1$ or $2\mathbf{Q}\equiv 0$ as in URu_2Si_2. In order to describe a finite-temperature transition into ordered state one can use a simple molecular-field approximation.[42,43] For this we write

$$\langle S_i^x \rangle = m_s e^{i\mathbf{Q}\mathbf{r}_i}, \tag{17}$$

where the dimensionless staggered magnetization m_s is determined by a self-consistency equation obtained from a single-site solution

$$m_s = \frac{2\mu^2 |\mathcal{J}_\mathbf{Q}| m_s}{\sqrt{\Delta^2 + 16\mu^4 \mathcal{J}_\mathbf{Q}^2 m_s^2}} \tanh \frac{\sqrt{\Delta^2 + 16\mu^4 \mathcal{J}_\mathbf{Q}^2 m_s^2}}{2T}. \tag{18}$$

The transition temperature obtained from the above equation is

$$\frac{\Delta}{T_N} = \ln \frac{\Delta_c + \Delta}{\Delta_c - \Delta}. \tag{19}$$

In the molecular-field approximation the transition temperature vanishes as $\Delta \to \Delta_c - 0$ in agreement with Eq. (16). At zero temperature the sublattice magnetization is

$$M_{s0} = 2\mu m_{s0} = \mu \sqrt{1 - \frac{\Delta^2}{\Delta_c^2}}, \tag{20}$$

whereas near T_N the antiferromagnetic moments follow the mean-field temperature dependence

$$M_s^2 \approx M_{s0}^2 \frac{\Delta^2}{T_N \Delta_c - \frac{1}{2}\Delta_c^2 + \frac{1}{2}\Delta^2} \frac{T_N - T}{T_N}. \tag{21}$$

The excitation spectrum in the ordered phase at zero temperature is found by introducing a staggered canting angle φ for the two sublattices.[46] In the mean-field approximation $\cos\varphi = \Delta/\Delta_c$. After transformation to the local (rotating) frame and application of Eq. (14) one finds

$$\omega_\mathbf{k} = 2\mu^2 |\mathcal{J}_\mathbf{Q}| \sqrt{1 + \frac{\Delta^2}{\Delta_c^2} \frac{\mathcal{J}_\mathbf{k}}{|\mathcal{J}_\mathbf{Q}|}}. \tag{22}$$

The above equation shows that upon approaching the Ising limit $\Delta \ll \Delta_c$, the dispersion of the longitudinal excitations is gradually diminished. For more details and discussion see the end of the subsection C.

Neutron scattering measurements on URu_2Si_2 yield a moderate value of the matrix element of the total angular momentum $\mu \simeq 1.2\mu_B$.[8] A simple explanation of small static moments would be, then, to assume that $(\Delta_c - \Delta) \ll \Delta$. According to Eq. (19) such an assumption also leads to a small transition temperature compared to the crystal-field level splitting $T_N \ll \Delta$, which is again in agreement with the experimental observation of $\Delta \simeq 10$ meV.[8] The above straightforward explanation of small ordered moments fails, however, to explain a large jump of the specific heat at T_N. Indeed, in the molecular-field approximation the specific heat jump at the transition temperature (19) is

$$\frac{\Delta C}{C} = 2T_N \frac{\Delta_c^2}{\Delta^2} \left| \frac{dm_s^2}{dT} \right|_{T_N}. \tag{23}$$

Using Eq. (21) we find in the limit $\Delta \to \Delta_c$

$$\frac{\Delta C}{C} \approx \frac{\Delta_c^2 - \Delta^2}{2\Delta_c^2} \ln \frac{\Delta_c + \Delta}{\Delta_c - \Delta}. \tag{24}$$

Taking $M_{s0} \approx 0.03\mu_B$, which implies that $(\Delta_c - \Delta)/\Delta_c \approx 3 \times 10^{-4}$, we find for the specific heat jump $\Delta C/C \approx 2.7 \times 10^{-3}$. Such a jump is three orders of magnitude smaller than the experimentally measured jump at the 17.5 K transition.[3] Corrections to the molecular-field approximation[44,45] do not significantly modify the jump ΔC. Consequently, it has been concluded that spontaneous ordering of local moments on uranium sites cannot explain the phenomenology of the antiferromagnetic transition in URu_2Si_2. In the next sections we shall consider the model (13) in the regime of induced local moments, that is $\Delta > \Delta_c = 2\mu^2 |\mathcal{J}_\mathbf{Q}|$ and $H_s \neq 0$.

B. Finite fields: Mean-field approximation

The mean-field ansatz for a sublattice magnetization in the presence of both uniform H and staggered H_s magnetic fields is given by

$$\langle S_i^x \rangle = m_s e^{i\mathbf{Q}\mathbf{r}_i} + m_0. \tag{25}$$

For a single spin, the mean-field Hamiltonian takes the following form:

$$\hat{\mathcal{H}}_{\mathrm{MF}} = -\Delta S_i^z - S_i^x [(2\mu H_s + 4\mu^2 |\mathcal{J}_\mathbf{Q}| m_s) e^{i\mathbf{Q}\mathbf{r}_i} + 2\mu H - 4\mu^2 \mathcal{J}_0 m_0], \tag{26}$$

where $\mathcal{J}_0 = \mathcal{J}_{\mathbf{k}=0}$. Calculating an equilibrium magnetization we find for two sublattices

$$m_s \pm m_0 = \frac{D_\pm}{\sqrt{\Delta^2 + 4D_\pm^2}} \tanh \frac{\sqrt{\Delta^2 + 4D_\pm^2}}{2T}, \tag{27}$$

$$D_\pm = \mu(H_s \pm H) + 2\mu^2 (|\mathcal{J}_\mathbf{Q}| m_s \mp \mathcal{J}_0 m_0).$$

Below, we focus on the case $\Delta > \Delta_c = 2\mu^2 |\mathcal{J}_\mathbf{Q}|$, when there is no magnetic ordering in the subsystem of local moments down to $T=0$ in the absence of both external and internal fields. For weak staggered field, linearization of Eq. (27) in H_s and m_s at $H=0$ yields

$$m_s = \frac{\mu H_s \tanh(\Delta/2T)}{\Delta - \Delta_c \tanh(\Delta/2T)}. \tag{28}$$

In accordance with the phenomenological formula (3) of Sec. II, weak local moments are proportional to the primary (SDW) order parameter. At zero temperature the dimensional staggered moments are

$$M_{s0} = 2\mu \frac{\mu H_s}{\Delta - \Delta_c}. \tag{29}$$

The above equation allows to estimate the staggered field in URu_2Si_2 from the available experimental data, see Sec. V.

The effect of a uniform field on induced local moments is considered, for simplicity, for $T=0$ only. In this case expansion of Eq. (27) to linear order in m_s and H_s yields

$$m_s = \frac{\mu H_s}{\Delta(1+4\mu^2\tilde{H}^2/\Delta^2)^{3/2}-\Delta_c}, \tag{30}$$

where an effective field $\tilde{H}=H-2\mu\mathcal{J}_0 m_0$ is determined self-consistently from

$$\tilde{H} = H - \frac{2\mu^2\mathcal{J}_0\tilde{H}}{(\Delta^2+4\mu^2\tilde{H}^2)^{1/2}}. \tag{31}$$

According to arguments of Sec. III, the SDW contribution to the magnetic Bragg peaks is negligible due to a small form factor. Then, the measured intensity of Bragg reflections is proportional to m_s^2. Suppression of an SDW order parameter with an external field can be described by a simple formula $\psi^2 \propto (1-H^2/H_c^2)$ or $H_s^2=H_{s0}^2(1-H^2/H_c^2)$, where $H_c \simeq 40$ T is a metamagnetic field in URu_2Si_2.[47] The magnetic Bragg peak intensity is

$$I_{\mathbf{Q}} \sim m_s^2 = \frac{\mu^2 H_{s0}^2(1-H^2/H_c^2)}{[\Delta(1+4\mu^2\tilde{H}^2/\Delta^2)^{3/2}-\Delta_c]^2}. \tag{32}$$

This zero-temperature result should be compared to the analogous formulas valid near T_m, which have been derived in the previous works[20,24] from the Landau free-energy functional. Though different in the details, the two limits exhibit an inflection point in $I_{\mathbf{Q}}(H)$. The staggered magnetization remains finite until H_c, when the primary-order parameter is suppressed to zero. The ordered moments are, however, substantially reduced compared to its zero-field value at significantly smaller magnetic field. Indeed, expanding Eqs. (31) and (32) to the first order in H^2 we obtain

$$\frac{m_s^2(H)}{m_s^2(0)} \approx 1 - H^2\left(\frac{1}{H_c^2} + \frac{12\mu^2\Delta}{(\Delta-\Delta_c)(\Delta+2\mu^2\mathcal{J}_0)^2}\right). \tag{33}$$

For the completeness we also note that the ferromagnetic component of the induced magnetic moments is given by

$$m_0 = \frac{\mu H}{\Delta + 2\mu^2\mathcal{J}_0} \tag{34}$$

for fields smaller than $H^*=(\Delta+2\mu^2\mathcal{J}_0)/2\mu$. Above this field the ferromagnetic component remains constant until a metamagnetic transition related to a crossing with higher energy crystal-field levels. The uniform component of the induced moments m_0 should be measurable from a magnetic contribution to the nuclear Bragg peaks.

C. Finite fields: Energy spectrum

We start with the case $H\neq 0$, $H_s=0$, since an effective H_s in URu_2Si_2 should be quite small. Partial polarization of magnetic moments (pseudo spins) along $\hat{z}$ ($\hat{x}$) axis is taken into account by rotation of pseudo spins from a laboratory frame to a local (primed) frame

$$S_i^x = S_i^{x'}\cos\varphi + S_i^{z'}\sin\varphi,$$

$$S_i^z = -S_i^{x'}\sin\varphi + S_i^{z'}\cos\varphi. \tag{35}$$

In the transformed frame and omitting primes the Hamiltonian (13) takes the following form:

$$\hat{\mathcal{H}} = 4\mu^2\sum_{\langle i,j\rangle}\mathcal{J}(ij)[S_i^xS_j^x\cos^2\varphi + S_i^zS_j^z\sin^2\varphi + (S_i^xS_j^z + S_i^zS_j^x)\sin\varphi\cos\varphi] - \sum_i[(\Delta\cos\varphi + 2\mu H\sin\varphi)S_i^z + (2\mu H\cos\varphi - \Delta\sin\varphi)S_i^x]. \tag{36}$$

The boson representation (14) of the pseudo-spin operators is applied to the above Hamiltonian and the rotation angle φ is determined from the condition of vanishing linear terms in a_i and $a_i^\dagger$

$$\Delta\tan\varphi + 2\mu^2\mathcal{J}_0\sin\varphi = 2\mu H. \tag{37}$$

At small fields $\varphi \approx 2\mu H/(\Delta+2\mu^2\mathcal{J}_0)$.

The harmonic part of the Hamiltonian (36) after the Fourier transformation becomes

$$\hat{\mathcal{H}}_2 = \sum_{\mathbf{k}} a_{\mathbf{k}}^\dagger a_{\mathbf{k}}[\Delta\cos\varphi + 2\mu H\sin\varphi - 2\mu^2\sin^2\varphi\mathcal{J}_0 + \mu^2\cos^2\varphi\mathcal{J}_{\mathbf{k}}] + \frac{1}{2}\mu^2\cos^2\varphi\mathcal{J}_{\mathbf{k}}(a_{\mathbf{k}}a_{-\mathbf{k}} + a_{\mathbf{k}}^\dagger a_{-\mathbf{k}}^\dagger). \tag{38}$$

The $\mathbf{k}$-independent term is simplified with the help of Eq. (37) to $\Delta/\cos\varphi$ and after applying the Bogoliubov transformation we obtain the following field dependence of the exciton spectrum:

$$\omega_{\mathbf{k}}^2 = \frac{\Delta^2}{\cos^2\varphi} + 2\mu^2\mathcal{J}_{\mathbf{k}}\Delta\cos\varphi. \tag{39}$$

The gap at $\mathbf{k}=\mathbf{Q}$ increases quadratically with magnetic field

$$\Delta_g^2(H) \approx \Delta(\Delta-\Delta_c) + \frac{2\mu^2H^2}{(\Delta+2\mu^2\mathcal{J}_0)^2}\Delta(2\Delta+\Delta_c). \tag{40}$$

The parabolic law for the field dependence of the gap has recently been measured in neutron scattering experiments.[24] For an arbitrary wave vector the field dependence of the exciton energy is

$$\omega_{\mathbf{k}}^2(H) \approx \omega_{\mathbf{k}}^2(0) + \frac{4\mu^2H^2\Delta}{(\Delta+2\mu^2\mathcal{J}_0)^2}[\Delta-\mu^2\mathcal{J}_{\mathbf{k}}]. \tag{41}$$

The field dependence changes its sign, i.e., the energy starts to decrease with magnetic field, for the wave vectors such that $\mu^2\mathcal{J}_{\mathbf{k}}>\Delta$. In terms of zero-field frequencies this is equivalent to $\omega_{\mathbf{k}}>\sqrt{3}\Delta$. In the region in the Brillouin zone where $\omega_{\mathbf{k}}\approx\sqrt{3}\Delta$ the field dependence of the spectrum becomes vanishingly small. Experimentally, a drastic change in the field dependence has been observed between $\mathbf{k}=\mathbf{Q}=(1,0,0)$ and $\mathbf{k}=(1.4,0,0)$. The present theory explains a qualitative difference in the field response of the two types of excitons. Further inelastic neutron measurements on URu_2Si_2 should allow a detailed comparison with our theory and extraction of microscopic parameters from experimental data.

If both staggered and uniform fields are present, the derivation of the spectrum becomes a bit more complicated. One has to explicitly introduce two types of bosons a_i and b_i for two antiferromagnetic sublattices and to calculate spectrum in the magnetic Brillouin zone, which is twice smaller than an original lattice Brillouin zone used above. The transformation to local (primed) axes from the laboratory frame is given by

$$S_i^x = S_i^{x'} \cos\varphi_i + S_i^{z'} e^{i\mathbf{Q}\mathbf{r}_i} \sin\varphi_i,$$

$$S_i^z = -S_i^{x'} e^{i\mathbf{Q}\mathbf{r}_i} \sin\varphi_i + S_i^{z'} \cos\varphi_i, \tag{42}$$

where two angles $\varphi_i=\varphi_1$, for $e^{i\mathbf{Q}\mathbf{r}_i}=1$ and $\varphi_i=\varphi_2$, for $e^{i\mathbf{Q}\mathbf{r}_i}=-1$ describe different response of the two sublattices. The angles are determined by

$$\Delta \tan\varphi_1 + 2\mu^2 \mathcal{J}_1 \sin\varphi_1 = 2\mu(H_s + H) + 2\mu^2 \mathcal{J}_2 \sin\varphi_2,$$

$$\Delta \tan\varphi_2 + 2\mu^2 \mathcal{J}_1 \sin\varphi_2 = 2\mu(H_s - H) + 2\mu^2 \mathcal{J}_2 \sin\varphi_1.$$

Here we defined separate summation of exchange constants over the same $\mathcal{J}_1=\Sigma_{i,j\in A}\mathcal{J}(ij)$ and the different sublattices $\mathcal{J}_2=\Sigma_{i\in A,j\in B}\mathcal{J}(ij)$.

Performing the same steps as in the case of $H_s=0$ we in the end find

$$\omega_{\mathbf{k}}^{\pm 2} = \frac{1}{2}(\omega_{1\mathbf{k}}^2 + \omega_{2\mathbf{k}}^2) \pm \sqrt{\frac{1}{4}(\omega_{1\mathbf{k}}^2 - \omega_{2\mathbf{k}}^2)^2 + 4\mu^4 \mathcal{J}_{2\mathbf{k}}^2 \Delta^2 \cos\varphi_1 \cos\varphi_2},$$

$$\omega_{1,2\mathbf{k}}^2 = \frac{\Delta^2}{\cos^2\varphi_{1,2}} + 2\mu^2 \mathcal{J}_{1\mathbf{k}} \Delta \cos\varphi_{1,2}. \tag{43}$$

Here, the Fourier transforms are given by $\mathcal{J}_{1\mathbf{k}}=\Sigma_{i,j\in A}\mathcal{J}(ij)e^{i\mathbf{k}\mathbf{r}_{ij}}$ and $\mathcal{J}_{2\mathbf{k}}=\Sigma_{i\in A,j\in B}\mathcal{J}(ij)e^{i\mathbf{k}\mathbf{r}_{ij}}$. The characteristic feature of this spectrum is a small jump between two branches of excitations $\omega_{\mathbf{k}}^+$ and $\omega_{\mathbf{k}}^-$ at the magnetic Brillouin zone boundary, where $\mathcal{J}_{2\mathbf{k}}\equiv 0$. In URu_2Si_2 ($H_s\neq 0$) such a jump is induced by external magnetic field $H\sim H_s$ and becomes negligible again for $H\gg H_s$, when the above expression Eq. (39) is valid.

Finally, let us comment on the longitudinal polarization of magnetic excitons detected experimentally.[8] In the harmonic approximation, the dynamic structure factor $S^{zz}(\mathbf{r},\tau)=\langle J_i^z(t)J_{i+\mathbf{r}}^z(t+\tau)\rangle$ is expressed via pseudo-spin operators as

$$S^{zz}(\mathbf{r},\tau) \approx 4\mu^2 \cos^2\varphi \langle S_i^x(t) S_{i+\mathbf{r}}^x(t+\tau)\rangle. \tag{44}$$

In a weakly polarized Van Vleck paramagnet for $\Delta\sim\Delta_c$ one has $\cos\varphi_{1,2}\approx 1$. Therefore, transverse "spin-wave-type modes" in the pseudo-spin representation correspond to longitudinal polarization of magnetic excitons. The omitted terms in Eq. (44), such as $\langle S_i^z S_{i+\mathbf{r}}^z\rangle$ and $\langle S_i^x S_{i+\mathbf{r}}^z\rangle$, describe a higher energy two-magnon continuum and its interaction with single-particle states. These terms do not modify the conclusion about longitudinal polarization of single-particle excitations. In the opposite limit $\Delta\ll\Delta_c$ in a phase with large antiferromagnetic moments $\cos\varphi_{1,2}\to 0$, and the longitudinal dynamic structure factor $S^{zz}(\mathbf{q},\omega)$ does not have contribution from magnetic excitons. This explains why the neutron scattering measurements[24] failed to observe the magnetic excitations above the first-order transition at $P_M=5$ kbar.

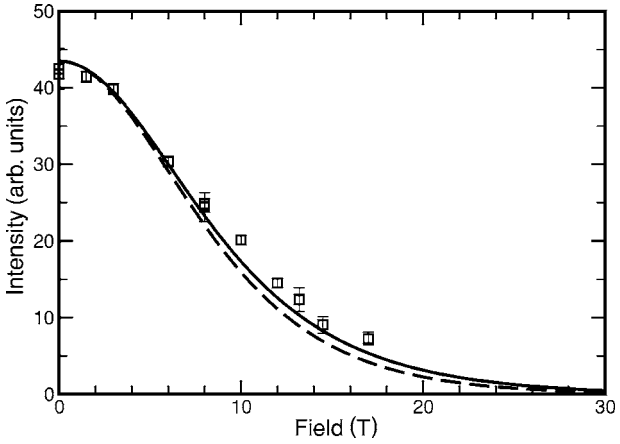

FIG. 2. Field dependence of the intensity of the antiferromagnetic Bragg peak at $\mathbf{Q}=(1,0,0)$. Points are the experimental data (see Ref. 24). Lines are theoretical curves described by Eq. (32) with $\Delta=6$ meV (full line) and $\Delta=3$ meV (dashed line).

V. COMPARISON WITH EXPERIMENT

Theoretical predictions of the above section can be directly compared with the available experimental data. Specifically, let us consider the field dependence of the intensity of the magnetic Bragg peak. The metamagnetic transition in URu_2Si_2 at $H_c\simeq 40$ T can be chosen as the critical field for the spin-density wave. The field dependence of the Bragg peak intensity described by Eqs. (31) and (32) is, then, determined by three microscopic parameters: Δ, $\Delta_c=2\mu^2|\mathcal{J}_{\mathbf{Q}}|$, and $2\mu^2\mathcal{J}_0$. The last two parameters are fixed by using the experimental data[24] for the excitation gap $\Delta_g=\sqrt{\Delta(\Delta-\Delta_c)}\approx 1.59$ meV and its dependence on applied magnetic field. In this way we are left with only one free parameter: the crystal-field splitting Δ.

The two theoretical curves for $\Delta=3$ meV ($\Delta_c=2.2$ meV and $2\mu^2\mathcal{J}_0=1.3$ meV) and $\Delta=6$ meV ($\Delta_c=5.57$ meV and $2\mu^2\mathcal{J}_0=2.9$ meV) are presented in Fig. 2 together with the experimental data.[24] Both curves exhibit behavior with an inflection point. The larger value of the gap gives better agreement with the experimental results. For $\Delta=6$ meV the top of the exciton band at $H=0$ calculated from Eq. (15) corresponds to $\omega_0\approx 7.3$ meV. The internal staggered field estimated from Eq. (29) in this case is $H_s\approx 0.08$ T, which is indeed much smaller than applied magnetic fields and justifies the used approximations.

If we further increase Δ, the theoretical dependence for $I_{\mathbf{Q}}(H)$ with the above two constraints practically saturates at the position given by $\Delta=6$ meV curve. Thus, while we can definitely exclude smaller values $\Delta<6$ meV for the crystal-field level splitting, the larger values $\Delta>6$ meV are equally possible. For example, for $\Delta=10$ meV, which has been suggested on the basis of the early neutron scattering measurements,[8] the parameters obtained from the fits are

Δ_c=9.7 meV, $2\mu^2\mathcal{J}_0$=4.9 meV, and $\omega_0 \approx 12.2$ meV. At present, there is no agreement on the value of ω_0 between the two groups of inelastic neutron measurements.[8,24,48] Additional precise neutron scattering investigation of URu_2Si_2 should greatly help to settle this dispute.

VI. CONCLUSIONS

We have presented a theoretical model to describe unusual magnetism in URu_2Si_2 below T_m=17.5 K, which combines tiny ordered moments $\mu \sim 0.03\mu_B$ with a large specific heat anomaly at the transition point. At ambient pressure, the transition is driven by an SDW instability in the itinerant subsystem, which also induces weak ordering of local moments on uranium sites. We argue that such a low-T_c spin-density wave has a small form factor and does not contribute significantly to the neutron scattering, which essentially probes the localized subsystem. Phenomenologically, the phase diagram of URu_2Si_2 is described by the two-order parameter functional (2), which is consistent with the first-order transition into a state with large antiferromagnetic moments. The microscopic origin of a strong repulsion between two-order parameters of the same symmetry needs further clarification. In our view such a behavior may result from a strong renormalization of the RKKY-type interaction between the local moments by a rather large SDW gap, which opens over a half of the Fermi surface.

In our discussion we have assumed, following the previous works,[8,17,18] that uranium ions are in the $^3H_4$ ground state. The validity of such an assumption needs further clarification. Also, the high field behavior with an itinerant electron metamagnetic transition[47] would be an interesting test for the dual model and its extension suggested in in the present work. Another open question is temperature evolution of the crystal-field excitations. We believe that the experimentally observed disappearance of the magnetic excitons above the transition temperature[8,24] is largely related to the closeness of two energy scales: T_m=17.5 K and Δ_g =1.6 meV.

The analysis presented in Sec. IV A may be also relevant to UPt_3, another heavy-fermion compound with tiny antiferromagnetic moments; for review see Ref. 49. This material does not have apparent anomalies in thermodynamic and kinetic properties at $T_m \approx 5$ K, though the neutron diffraction experiments have detected small antiferromagnetic moments $\mu \sim 0.02\mu_B$. In a possible scenario for UPt_3, there is no SDW instability in the conduction subsystem. The phase transition is driven by the RKKY or the superexchange interaction between local moments, which only slightly exceeds the critical value for zero-temperature antiferromagnetic ordering determined by a crystal-field level splitting. While the crystal level structure is not precisely known for UPt_3, the estimates for the specific heat anomaly given in the end of Sec. IV A should be generally valid. Thus, the small ordered antiferromagnetic moments can be reconciled with the absence of large anomalies at the transition point. The pressure effect on antiferromagnetic ordering in UPt_3 also agrees with Eqs. (19) and (20), which predict a much faster square-root suppression of zero-temperature moments compared to a slow logarithmic decrease of the transition temperature.

ACKNOWLEDGMENTS

It is a pleasure to express our gratitude to F. Bourdarot and B. Fåk for the numerous stimulating discussions. We would also like to thank M. R. Norman and T. M. Rice for valuable comments.

[1] T. T. M. Palstra, A. A. Menovsky, J. van den Berg, A. J. Dirkmaat, P. H. Kes, G. J. Nieuwenhuys, and J. A. Mydosh, Phys. Rev. Lett. **55**, 2727 (1985).
[2] W. Schlabitz, J. Baumann, B. Pollit, U. Rauchschwalbe, H. M. Meyer, U. Ahlheim, and C. D. Bredl, Z. Phys. B: Condens. Matter **62**, 171 (1986).
[3] M. B. Maple, J. W. Chen, Y. Dalichaouch, T. Kohara, C. Rossel, M. S. Torikachvili, M. W. McElfresh, and J. D. Thompson, Phys. Rev. Lett. **56**, 185 (1986).
[4] T. T. M. Palstra, A. A. Menovsky, and J. A. Mydosh, Phys. Rev. B **33**, R6527 (1986).
[5] A. de Visser, F. E. Kayzel, A. A. Menovsky, J. J. M. France, J. van den Berg, and G. J. Nieuwenhuys, Phys. Rev. B **34**, R8168 (1986).
[6] C. Broholm, J. K. Kjems, W. J. L. Buyers, P. Matthews, T. T. M. Palstra, A. A. Menovsky, and J. A. Mydosh, Phys. Rev. Lett. **58**, 1467 (1987).
[7] T. E. Mason, B. D. Gaulin, J. D. Garrett, Z. Tun, W. J. L. Buyers, and E. D. Isaacs, Phys. Rev. Lett. **65**, 3189 (1990).
[8] C. Broholm, H. Lin, P. T. Matthews, T. E. Mason, W. J. L. Buyers, M. F. Collins, A. A. Menovsky, J. A. Mydosh, and J. K. Kjems, Phys. Rev. B **43**, 12809 (1991).
[9] B. Fåk, C. Vettier, J. Flouquet, F. Bourdarot, S. Raymond, A. Vernière, P. Lejay, Ph. Boutrouille, N. R. Bernhoeft, S. T. Bramwell, R. A. Fisher, and N. E. Phillips, J. Magn. Magn. Mater. **154**, 339 (1996).
[10] E. D. Isaacs, D. B. McWhan, R. N. Kleiman, D. J. Bishop, G. E. Ice, P. Zschack, B. D. Gaulin, T. E. Mason, J. D. Garrett, and W. J. L. Buyers, Phys. Rev. Lett. **65**, 3185 (1990).
[11] G. J. Nieuwenhuys, Phys. Rev. B **35**, 5260 (1987).
[12] L. P. Gor'kov, Europhys. Lett. **16**, 303 (1991); L. P. Gor'kov and A. Sokol, Phys. Rev. Lett. **69**, 2586 (1992).
[13] A. P. Ramirez, P. Coleman, P. Chandra, E. Brück, A. A. Menovsky, Z. Fisk, and E. Bucher, Phys. Rev. Lett. **68**, 2680 (1992).
[14] V. Barzykin and L. P. Gor'kov, Phys. Rev. Lett. **70**, 2479 (1993).
[15] D. F. Agterberg and M. B. Walker, Phys. Rev. B **50**, 563 (1994).
[16] P. Santini and G. Amoretti, Phys. Rev. Lett. **73**, 1027 (1994); M. B. Walker and W. J. L. Buyers, *ibid.* **74**, 4097 (1995); P. Santini and G. Amoretti, *ibid.* **74**, 4098 (1995).
[17] A. E. Sikkema, W. J. L. Buyers, I. Affleck, and J. Gan, Phys. Rev. B **54**, 9322 (1996).
[18] Y. Okuno and K. Miyake, J. Phys. Soc. Jpn. **67**, 2469 (1998).
[19] H. Ikeda and Y. Ohashi, Phys. Rev. Lett. **81**, 3723 (1998).
[20] N. Shah, P. Chandra, P. Coleman, and J. A. Mydosh, Phys. Rev. B

61, 564 (2000).
[21] P. Chandra, P. Coleman, J. A. Mydosh, and V. Tripathi, Nature (London) **417**, 831 (2002); P. Chandra, P. Coleman, and J. A. Mydosh, Physica B **312–313**, 397 (2002).
[22] A. Kiss and P. Fazekas, cond-mat/0411029 (unpublished).
[23] I. A. Fomin (unpublished).
[24] F. Bourdarot, B. Fåk, K. Habicht, and K. Prokes, Phys. Rev. Lett. **90**, 067203 (2003).
[25] H. Amitsuka, M. Sato, N. Metoki, M. Yokoyama, K. Kuwahara, T. Sakakibara, H. Morimoto, S. Kawarazaki, Y. Miyako, and J. A. Mydosh, Phys. Rev. Lett. **83**, 5114 (1999).
[26] G. Motoyama, T. Nishioka, and N. K. Sato, Phys. Rev. Lett. **90**, 166402 (2003).
[27] F. Bourdarot, B. Fåk, V. P. Mineev, M. E. Zhitomirsky, N. Kernavanois, S. Raymond, P. Burlet, F. Lapierre, P. Lejay, and J. Flouquet, cond-mat/0312206, Physica B (to be published).
[28] K. Matsuda, Y. Kohori, T. Kohara, K. Kuwahara, and H. Amitsuka, Phys. Rev. Lett. **87**, 087203 (2001).
[29] K. Matsuda, Y. Kohori, T. Kohara, K. Kuwahara, and T. Matsumoto, J. Phys.: Condens. Matter **15**, 2363 (2003).
[30] M. R. Norman, T. Oguchi, and A. J. Freeman, Phys. Rev. B **38**, 11193 (1988).
[31] M. E. Zhitomirsky and V.-H. Dao, Phys. Rev. B **69**, 054508 (2004).
[32] R. A. Fisher, S. Kim, Y. Wu, N. E. Phillips, M. W. McElfresh, M. S. Torikachvili, and M. B. Maple, Physica B **163**, 419 (1990).
[33] H. Ohkuni, Y. Inada, Y. Tokiwa, K. Sakurai, R. Settai, T. Honma, Y. Haga, E. Yamamoto, Y. Onuki, H. Yamagami, S. Takahashi, and T. Yanagisawa, Philos. Mag. B **79**, 1045 (1999).
[34] S. A. M. Mentink, T. E. Mason, S. Süllow, G. J. Nieuwenhuys, A. A. Menovsky, J. A. Mydosh, and J. A. A. J. Perenboom, Phys. Rev. B **53**, R6014 (1996).
[35] N. H. van Dijk, F. Bourdarot, J. C. P. Klaasse, I. H. Hagmusa, E. Brück, and A. A. Menovsky, Phys. Rev. B **56**, 14493 (1997).
[36] M. Jaime, K. H. Kim, G. Jorge, S. McCall, and J. A. Mydosh, Phys. Rev. Lett. **89**, 287201 (2002).
[37] R. H. McKenzie, cond-mat/9706235 (unpublished).
[38] G. Grüner, *Density Waves in Solids* (Perseus, Cambridge, MA, 1994).
[39] S. Skalski, O. Betbeder-Matibet, and P. R. Weiss, Phys. Rev. **136**, A1500 (1964).
[40] C. M. Varma, Phys. Rev. Lett. **55**, 2723 (1985).
[41] M. R. Norman, Phys. Rev. Lett. **59**, 232 (1987).
[42] B. Bleaney, Proc. R. Soc. London, Ser. A, **276**, 19 (1963).
[43] B. Grover, Phys. Rev. **140**, A1944 (1965).
[44] Y.-L. Yang and B. R. Cooper, Phys. Rev. **172**, 539 (1968); **185**, 696 (1969).
[45] M. A. Klenin and J. A. Hertz, Phys. Rev. B **14**, 3024 (1976).
[46] J. Jensen and A. R. Mackintosh, *Rare Earth Magnetism: Structure and Excitations* (Clarendon, Oxford, 1991).
[47] N. Harrison, M. Jaime, and J. A. Mydosh, Phys. Rev. Lett. **90**, 096402 (2003).
[48] F. Bourdarot, Ph.D. thesis, unpublished (1994).
[49] N. H. van Dijk, P. Rodière, B. Fåk, A. Huxley, and J. Flouquet, Physica B **319**, 220 (2002).